

# Toward the Oxidation of the Phenyl Radical and Prevention of PAH Formation in Combustion Systems

Dorian S. N. Parker and Ralf I. Kaiser\*

Department of Chemistry, University of Hawaii at Manoa, Honolulu, Hawaii 96822, United States

Tyler P. Troy, Oleg Kostko, and Musahid Ahmed\*

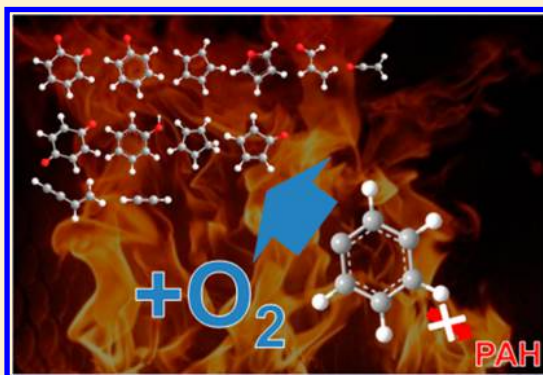
Chemical Sciences Division, Lawrence Berkeley National Laboratory, Berkeley, California 94720, United States

Alexander M. Mebel\*

Department of Chemistry and Biochemistry, Florida International University, Miami, Florida 33199, United States

**ABSTRACT:** The reaction of the phenyl radical ( $C_6H_5$ ) with molecular oxygen ( $O_2$ ) plays a central role in the degradation of poly- and monocyclic aromatic radicals in combustion systems which would otherwise react with fuel components to form polycyclic aromatic hydrocarbons (PAHs) and eventually soot. Despite intense theoretical and experimental scrutiny over half a century, the overall reaction channels have not all been experimentally identified. Tunable vacuum ultraviolet photoionization in conjunction with a combustion simulating chemical reactor uniquely provides the complete isomer specific product spectrum and branching ratios of this prototype reaction. In the reaction of phenyl radicals and molecular oxygen at 873 K and 1003 K, *ortho*-benzoquinone (*o*- $C_6H_4O_2$ ), the phenoxy radical ( $C_6H_5O$ ), and cyclopentadienyl radical ( $C_5H_5$ ) were identified as primary products formed through emission of atomic hydrogen, atomic oxygen and carbon dioxide.

Furan ( $C_4H_4O$ ), acrolein ( $C_3H_4O$ ), and ketene ( $C_2H_2O$ ) were also identified as primary products formed through ring opening and fragmentation of the 7-membered ring 2-oxepinoxy radical. Secondary reaction products *para*-benzoquinone (*p*- $C_6H_4O_2$ ), phenol ( $C_6H_5OH$ ), cyclopentadiene ( $C_5H_6$ ), 2,4-cyclopentadienone ( $C_5H_4O$ ), vinylacetylene ( $C_4H_4$ ), and acetylene ( $C_2H_2$ ) were also identified. The pyranil radical ( $C_5H_5O$ ) was not detected; however, electronic structure calculations show that it is formed and isomerizes to 2,4-cyclopentadienone through atomic hydrogen emission. In combustion systems, barrierless phenyl-type radical oxidation reactions could even degrade more complex aromatic radicals. An understanding of these elementary processes is expected to lead to a better understanding toward the elimination of carcinogenic, mutagenic, and environmentally hazardous byproducts of combustion systems such as PAHs.



## I. INTRODUCTION

The combustion of fossil fuel drives the economy of our planet and delivers energy by oxidation of aliphatic, alicyclic, and aromatic hydrocarbons. Ideally, this process leads solely to carbon dioxide ( $CO_2$ ) and water ( $H_2O$ ). However, in “real” combustion systems, in competition with these oxidation reactions are formation routes to carcinogenic, mutagenic, and environmentally detrimental species, polycyclic aromatic hydrocarbons (PAHs),<sup>1,2</sup> and soot particles.<sup>3,4</sup> These pathways involve reactions of resonantly stabilized free radicals (RSFRs) like propargyl ( $C_3H_3$ ) and aromatic radicals (ARs), such as the phenyl radical with unsaturated hydrocarbons.<sup>5–7</sup> Alternatively, in combustion environments, phenyl radicals also react with molecular oxygen, a key reaction that removes these radicals from PAH formation routes. At temperatures higher than 1000 K, this reaction is initiated by forming a rovibrationally excited

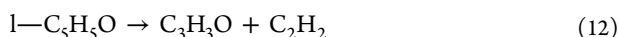
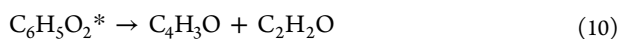
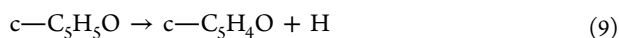
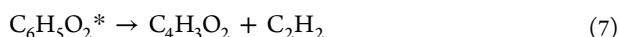
peroxybenzene radical ( $C_6H_5O_2$ )\* (1), that emits an oxygen atom leading to the phenoxy radical ( $C_6H_5O$ ) (2).<sup>8–11</sup> The formation of the phenoxy radical ( $C_6H_5O$ ) has also been observed as the primary product via crossed molecular beam experiments in the single collision regime at high temperatures.<sup>12–14</sup> Below 1000 K, based on kinetics studies, it has been postulated, that an addition-stabilization process yields the peroxybenzene radical ( $C_6H_5O_2$ ) as the primary product.<sup>10</sup>

**Special Issue:** 100 Years of Combustion Kinetics at Argonne: A Festschrift for Lawrence B. Harding, Joe V. Michael, and Albert F. Wagner

**Received:** September 10, 2014

**Revised:** October 27, 2014

Theoretical investigations have predicted the isomerization of the peroxybenzene radical ( $C_6H_5O_2$ ) with insertion of one of the oxygen atoms into the ring to form a seven-membered ring radical 2-oxepinoxy ( $C_6H_5O_2$ ).<sup>8,15,16</sup> Kinetics experiments on the oxidation of phenyl radicals observed the formation of *para*-benzoquinone ( $C_6H_4O_2$ ) (3) through atomic hydrogen emission.<sup>17,18</sup> Theoretical investigations predict further the formation of the cyclopentadienyl ( $c-C_5H_5$ ) radical by carbon monoxide (CO) loss from the phenoxy radical (4)<sup>8,10</sup> or through carbon dioxide ( $CO_2$ ) emission (5) from benzoquinone.<sup>19</sup> Formation routes to pyranyl ( $c-C_5H_5O$ ) plus carbon monoxide (6) and 2-oxo-2,3-dihydrofuran-4-yl ( $c-C_4H_3O_2$ ) plus acetylene (7) through the decomposition of the seven-membered ring radical 2-oxepinoxy ( $C_6H_5O_2$ )<sup>8,15</sup> or via oxidation by another oxygen molecule<sup>16</sup> are also proposed. Ring opening of the 2-oxepinoxy radical ( $C_6H_5O_2$ ) can form a 2,4-cyclopentadienone ( $c-C_5H_5O$ ) radical by carbon monoxide (CO) emission (8).<sup>15</sup> The 2,4-cyclopentadienone ( $c-C_5H_5O$ ) radical can emit a hydrogen atom yielding 2,4-cyclopentadienone ( $C_5H_4O$ ) (9). From experimental studies of benzene oxidation using turbulent flow reactors, Glassman et al. proposed the observed 2,4-cyclopentadienone ( $C_5H_4O$ ) was possibly from a secondary reaction of cyclopentadienyl with molecular oxygen.<sup>20</sup> The opening of the 2-oxepinoxy ( $C_6H_5O_2$ ) ring leads to a number of linear dioxo radicals such as the 1,6-dioxo-3,5-hexadienyl ( $C_6H_5O_2$ ) radical, which can subsequently fragment to yield polycarbon monoxides like 2-oxo-2,3-dihydrofuran-4-yl ( $C_4H_3O$ ) and ketene ( $C_2H_2O$ ) (10).<sup>15</sup> Emission of a  $C_2HO$  radical from 1,6-dioxo-3,5-hexadienyl ( $C_6H_5O_2$ ) radical leads to furan ( $C_4H_4O$ ) (11), or emission of carbon monoxide leads to a linear  $C_5H_5O$  molecule that subsequently fragments to an acrolein ( $C_3H_3O$ ) radical plus acetylene (12). Hydrogen addition to ( $C_3H_3O$ ) or abstraction from another hydrocarbon can form the stable molecule acrolein ( $C_3H_4O$ ). The fragmentation pattern continues for the polycarbon monoxide intermediates emitting a second carbon monoxide to form a  $C_4H_5$  intermediate (13) that can then dissociate to acetylene ( $C_2H_2$ ) and the vinyl radical ( $C_2H_3$ ) (14)<sup>15</sup> or alternatively can emit a hydrogen atom to form vinylacetylene ( $C_4H_4$ ) (15).<sup>21</sup> The following reactions 1–15 are from previous investigations on phenyl radical plus oxygen reaction:



Tokmakov et al. investigated the  $C_6H_5O_2$  potential energy surface (PES) to provide a comprehensive view of the multiple reaction channels investigated for the phenyl plus molecular oxygen reaction.<sup>9</sup> The authors proposed that feasible reaction pathways exist to the following products, phenoxy radical ( $C_6H_5O$ ), benzoquinone (*p*-/*o*- $C_6H_4O_2$ ), the cyclopentadienyl radical ( $C_5H_5$ ), pyranyl ( $C_5H_5O$ ), and 2-oxo-2,3-dihydrofuran-4-yl ( $C_4H_3O$ ). The most recent RRKM-ME calculations of product branching ratios in the temperature range of 1500–2500 K and pressures from 0.01 to 10 atm showed that the dominant reaction channel (>82%) leads to the phenoxy radical product and its contribution increases with temperature. Chemically activated phenoxy radical either decomposes to the cyclopentadienyl plus CO or undergoes thermal equilibration, where the relative yields of the decomposition/equilibration products strongly depend on temperature and pressure, with a temperature growth favoring decomposition and an increase in pressure favoring equilibration. At lower temperatures, the reaction was also predicted to yield significant amounts of pyranyl ( $C_5H_5O$ ) plus CO, cyclopentadienyl ( $C_5H_5$ ) plus CO, and *o*-benzoquinone (*o*- $C_6H_4O_2$ ) plus H.<sup>22</sup> However, despite the importance of the title reaction in combustion chemistry as a defacto PAH inhibitor, these predictions have not been verified experimentally. This is mainly due to the difficulties in probing all reaction products simultaneously. Therefore, a comprehensive experimental determination of the degradation pathways of the phenyl radical by molecular oxygen has remained elusive to date.

In this article, we present the results of the multichannel reaction of the phenyl radical with molecular oxygen explored experimentally under simulated combustion conditions. By exploiting the versatile detection technique of fragment-free single photon ionization coupled with mass spectroscopic detection of the photoionized products,<sup>23–27</sup> this study provides compelling evidence for the formation of primary reaction products [*o*-benzoquinone ( $C_6H_4O_2$ ), the cyclopentadienyl radical ( $C_5H_5$ ), and the phenoxy radical ( $C_6H_5O$ ), furan ( $C_4H_4O$ ), acrolein ( $C_3H_4O$ ), and ketene ( $C_2H_2O$ )], and higher-order products [*p*-benzoquinone ( $C_6H_4O_2$ ), phenol ( $C_6H_5OH$ ), cyclopentadiene ( $C_5H_6$ ), 2,4-cyclopentadienone ( $C_5H_4O$ ), vinylacetylene ( $C_4H_4$ ), and acetylene ( $C_2H_2$ )]. This reaction represents the prototype system of a whole reaction class, in which aromatic radicals can be degraded via reactions with molecular oxygen in combustion systems, eventually leading to an understanding of the elimination of toxic PAHs in the combustion of fossil fuel.

## II. EXPERIMENTAL SECTION

The experiments were conducted at the Chemical Dynamics Beamline (9.0.2.) at the Advanced Light Source (ALS) exploiting a resistively heated high-temperature “chemical reactor” incorporated into a molecular beam vacuum chamber equipped with a Wiley–McLaren reflectron time-of-flight mass spectrometer (ReTOF).<sup>23–27</sup> Phenyl radicals were generated in situ under combustion relevant conditions (temperature, pressure) via pyrolysis of nitrosobenzene ( $C_6H_5NO$ ; Aldrich; 99.5+ %) seeded at levels of less than 0.1% in molecular oxygen ( $O_2$ ; Praxair; 99.99%) by expanding the mixture at a backing

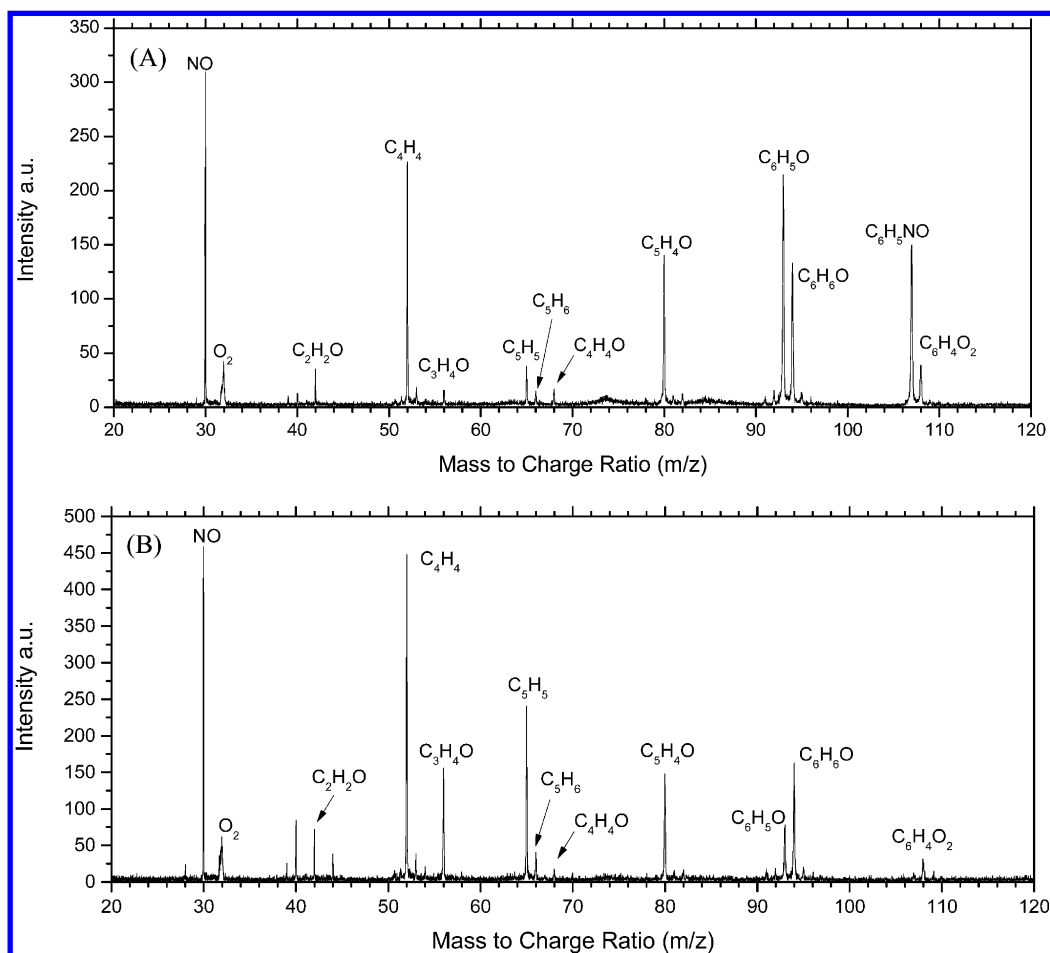


**Figure 1.** Mass spectra of the products of the phenyl–oxygen pyrolytic reaction recorded at a photon energy of 10.50 eV, (A) 873 K and (B) 1003 K.

pressure of about 300 Torr through a 0.1 mm orifice via a resistively heated silicon carbide (SiC) tube (1 mm inner diameter) operating at 873 and 1003  $\pm$  150 K. The limited precision of the temperature is accounted for by changes in conductance of the silicon carbide rod, and the thermal contact of the type C thermocouple. Note that molecular oxygen acts not only as a seeding gas but also as a reactant with the pyrolytically generated phenyl radicals. The continuous molecular beam generated in this process passes a 2 mm diameter skimmer located 10 mm downstream; this supersonic beam then enters the detection chamber, which houses the ReTOF mass spectrometer. Quasi-continuous tunable vacuum ultraviolet (VUV) radiation from the ALS interrogates the neutral molecular beam in the extraction region of the ReTOF mass spectrometer 55 mm downstream from the heated nozzle. Note that photo ionization via VUV radiation benefits from quasi fragment free ionization, a soft ionization method compared to traditional electron impact ionization. The ions generated are extracted and directed toward the ReTOF, which houses a microchannel plate detector (MCP). Signal from the MCP is digitized using a multichannel scaler. Photoionization efficiency (PIE) curves were obtained by integrating the signal collected at a specific mass-to-charge ( $m/z$ ) selected for the species of interest over the range of photon energies from 8.00 to 11.00 eV in 0.05 eV increments and normalized to the photon flux.

### III. RESULTS

For the reaction of phenyl radicals with molecular oxygen, a characteristic mass spectrum collected at 10.50 eV is shown in Figure 1A for reactions conducted at 873 K and Figure 1B for 1003 K. The nozzle was run at an oxygen backing pressure of 300 Torr. The mass spectra depict product peaks at  $m/z$  26 ( $C_2H_2^+$ ), 42 ( $C_2H_2O^+$ ), 52 ( $C_4H_4^+$ ), 56 ( $C_3H_4O^+$ ), 65 ( $C_5H_5^+$ ), 66 ( $C_5H_6^+$ ), 68 ( $C_4H_4O^+$ ), 80 ( $C_5H_4O^+$ ), 93 ( $C_6H_5O^+$ ), 94 ( $C_6H_6O^+$ ), and 108 ( $C_6H_4O_2^+$ ). Blank spectra were recorded for neat nitrosobenzene and oxygen, respectively, in separate experiments and exhibit none of the peaks identified as products in the phenyl–oxygen experiment. The corresponding photoionization efficiency curves (PIE) for the products are shown in Figures 2 and 3 for the 873 and 1003 K experiments, respectively, reporting the intensities of the specific ion versus the photon energy. Each PIE depicted in Figures 2 and 3 by the black line is the average of three separate PIE scans, along with a shaded area indicating the error boundaries.

In the 873 and 1003 K experiments, signals at  $m/z$  108 are reflected in PIE curves (Figures 2A and 3A) that are well-matched by a composite of reference PIE curves (purple line) for *p*-benzoquinone (blue line),<sup>28</sup> *o*-benzoquinone (red line),<sup>28</sup> and the <sup>13</sup>C counterpart of the parent molecule nitrosobenzene (green line) that is also observed at  $m/z$  107 (Figure 1A). Under our experimental conditions for the 873 K experiment, the parent is not fully pyrolyzed as seen from the mass peak at

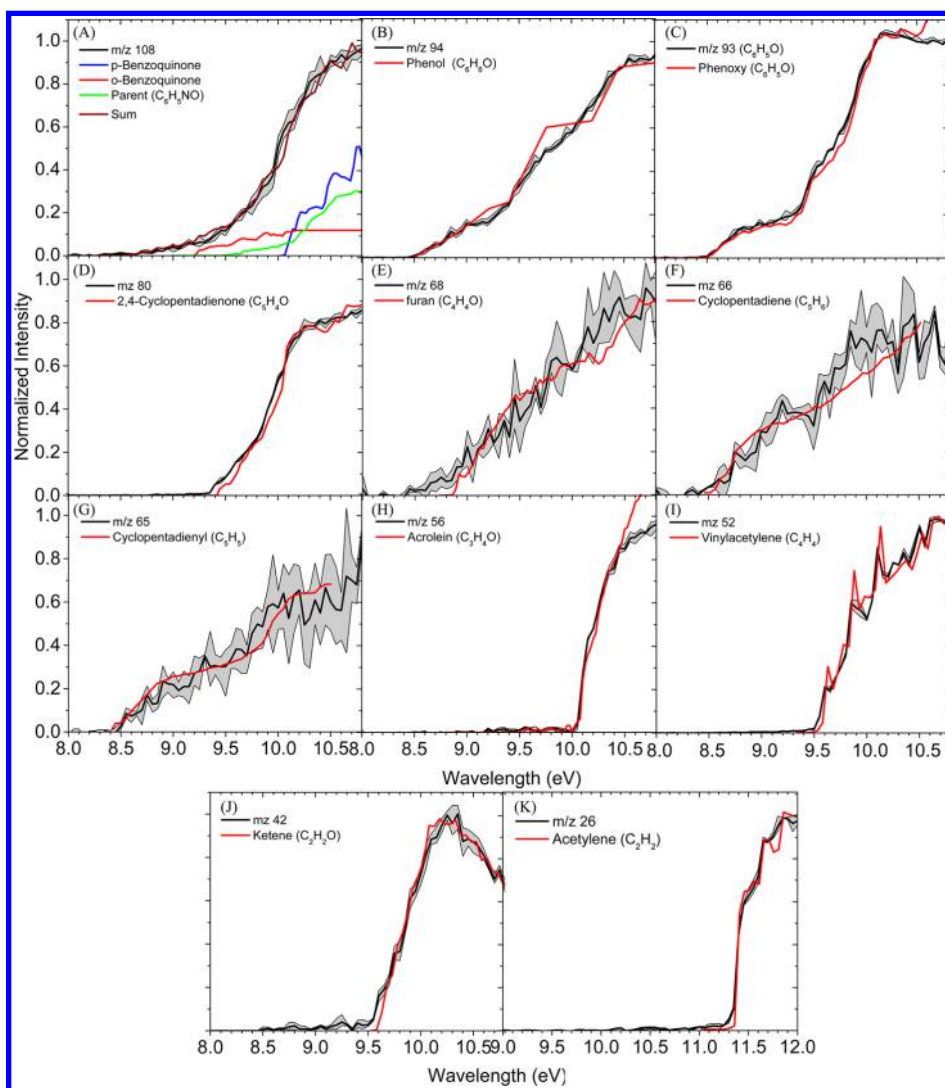


**Figure 2.** Experimentally obtained photoionization energy curves (PIE) recorded at 873 K at  $m/z = 108, 94, 93, 80, 68, 66, 65, 56, 52, 42,$  and  $26$ , shown as the black line along with experimental errors defined as the gray area. Reference PIE curves for each  $m/z$  ratio are shown as primary color (red, green, and blue) lines with the sum of the composite PIEs as the brown line.

$m/z$  107; a fraction of the signal at 108 originates from  $^{13}\text{C}$  nitrosobenzene ( $^{13}\text{C}_5\text{H}_5\text{NO}$ ). In the 1003 K experiment, the parent is almost fully pyrolyzed and the fit is achieved with no contribution from  $^{13}\text{C}$  nitrosobenzene ( $^{13}\text{C}_5\text{H}_5\text{NO}$ ). Here, the *o*-benzoquinone isomer has an onset at 9.2 eV and the *p*-benzoquinone at 10.0 eV.

The PIEs for  $m/z$  94 and 93 (Figures 2B, 3B, 2C, and 3C) are well-matched by the PIE for phenol ( $\text{C}_6\text{H}_5\text{OH}$ )<sup>29</sup> and by the phenoxy radical ( $\text{C}_6\text{H}_5\text{O}$ ), respectively. The PIE for phenol shows an onset at 9.5 eV and plateaus after 10.5 eV. In the present study, the phenoxy radical reference PIE was obtained by generating the radical through pyrolysis of allyl phenyl ether ( $\text{C}_3\text{H}_5\text{OC}_6\text{H}_5$ ) at 300 Torr and 873 K, a formation route to the phenoxy radical that has been well-documented.<sup>30</sup> Here, the phenoxy radical shares the same onset as phenol and sharply rises at 9.4 eV. The PIE of  $m/z$  80 (Figures 2D and 3D) is a very good match to the calculated PIE for 2,4-cyclopentadienone ( $\text{C}_5\text{H}_4\text{O}$ ), with an onset of 9.4 eV.<sup>29</sup> The signal at  $m/z$  68 (Figure 2E and 3E) although weak could be fit with experimental reference PIE's for furan ( $\text{C}_4\text{H}_4\text{O}$ ).<sup>31</sup> Here the signal is weak but shares the same rise profile as the reference.

In the 873 K experiment, signal at  $m/z$  65 (Figure 2G) has been assigned to the cyclopentadienyl radical (*c*- $\text{C}_5\text{H}_5$ ) due to its good match with the experimental reference PIEs (red line)<sup>32</sup> after subtraction of a dissociative ionization signal with onsets of 8.5 eV.<sup>33</sup> The raw PIE for  $m/z$  65 depicted a strong exponential increase at about 10 eV, which for a hydrocarbon reactant with molecular formula  $\text{C}_5\text{H}_5$  is an unfeasibly high ionization energy and therefore indicates dissociative ionization. The dissociative ionization of phenoxy radical forming cyclopentadienyl has been reported in the photodissociation of anisole to form phenoxy radicals.<sup>33</sup> We found that in the pyrolysis of allylphenyl ether to form the phenoxy radical, a signal at  $m/z$  65 is observed with an onset at about 10 eV and depicts a strong exponential increase. The PIE shown in Figure 2G is the result of subtraction of this exponential rise at 10 eV, found in the generation of the phenoxy radical from allylphenyl ether pyrolysis, from the raw PIE collected from the reaction of phenyl with molecular oxygen. In the 1003 K experiment, the phenoxy radical contribution is significantly reduced, while the cyclopentadienyl signal significantly increased. As a result no dissociative ionization signal was found at 10 eV, and the PIE shown in Figure 3G is a good fit to the reference PIE for the

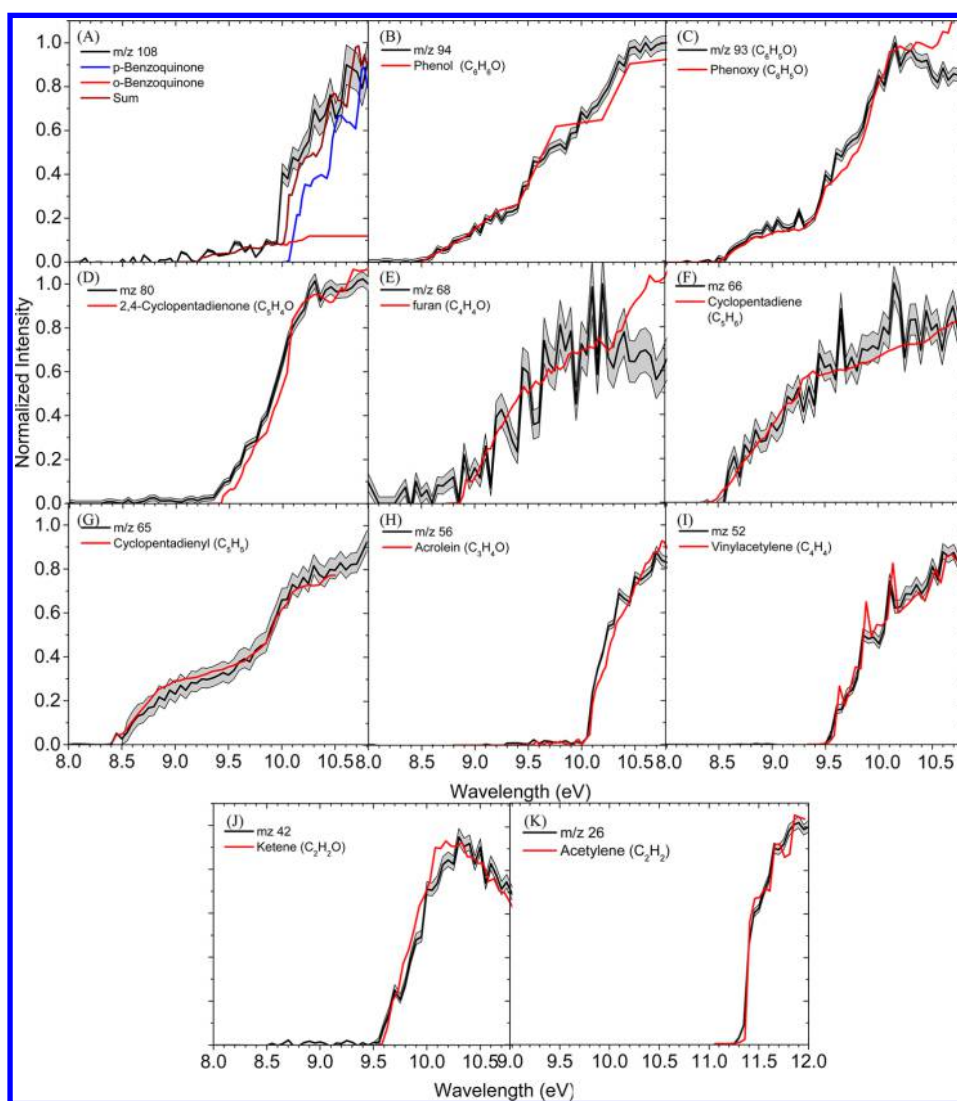


**Figure 3.** Experimentally obtained photoionization energy curves (PIE) recorded at 1003 K at  $m/z = 108, 94, 93, 80, 68, 66, 65, 56, 52, 42,$  and  $26$ , shown as the black line along with experimental errors defined as the gray area. Reference PIE curves for each  $m/z$  ratio are shown as primary color (red, green, and blue) lines with the sum of the composite PIEs as the brown line.

**Table 1. Branching Ratios of Species Formed in the Reaction of Phenyl with Oxygen Utilizing a Chemical Reactor at 300 Torr, 873 and 1003 K**

mass-to-charge ratio	name	molecular formula	branching ratio (%)		ratio between 873 and 1003 K branching ratios
			873 K	1003 K	
108	<i>o</i> -benzoquinone <sup>28</sup>	<i>o</i> -C <sub>6</sub> H <sub>4</sub> O <sub>2</sub>	0.54 ± 0.01	0.21 ± 0.01	0.39
108	<i>p</i> -benzoquinone <sup>28</sup>	<i>p</i> -C <sub>6</sub> H <sub>4</sub> O <sub>2</sub>	2.62 ± 0.05	0.93 ± 0.02	0.35
94	phenol <sup>40</sup>	C <sub>6</sub> H <sub>6</sub> O	10.99 ± 0.22	5.08 ± 0.10	0.46
93	phenoxy <sup>33</sup>	C <sub>6</sub> H <sub>5</sub> O	25.16 ± 0.50	3.90 ± 0.08	0.16
80	2,4-cyclopentadiene-1-one <sup>29</sup>	C <sub>5</sub> H <sub>4</sub> O	18.50 ± 0.18	9.04 ± 0.09	0.49
68	furan <sup>31</sup>	C <sub>4</sub> H <sub>4</sub> O	4.48 ± 0.45	1.39 ± 0.14	0.31
66	1,3-cyclopentadiene <sup>31</sup>	C <sub>5</sub> H <sub>6</sub>	4.87 ± 0.49	3.85 ± 0.38	0.79
65	cyclopentadienyl <sup>32</sup>	C <sub>5</sub> H <sub>5</sub>	6.66 ± 0.83	30.47 ± 3.81	4.58
56	acrolein <sup>35</sup>	C <sub>3</sub> H <sub>4</sub> O	6.00 ± 0.06	15.31 ± 0.15	2.55
52	vinylacetylene <sup>34</sup>	C <sub>4</sub> H <sub>4</sub>	14.03 ± 0.14	17.88 ± 0.18	1.27
42	ketene <sup>31</sup>	C <sub>2</sub> H <sub>2</sub> O	3.73 ± 0.11	5.27 ± 0.16	1.41
26	acetylene <sup>34</sup>	C <sub>2</sub> H <sub>2</sub>	2.43 ± 0.02	6.68 ± 0.07	2.75

cyclopentadienyl radical (*c*-C<sub>5</sub>H<sub>5</sub>) (red line).<sup>32</sup> The pent-1-en-4-yn-3-yl radical (65 u), which has a PIE onset of 7.88 eV, is clearly not formed under our experimental conditions.<sup>29</sup>

In the 873 K experiment, the PIE at  $m/z 66$  (Figure 2F) is attributed to cyclopentadiene (*c*-C<sub>5</sub>H<sub>6</sub>) as shown by the match to its experimental reference PIE (red lines).<sup>32</sup> In a similar

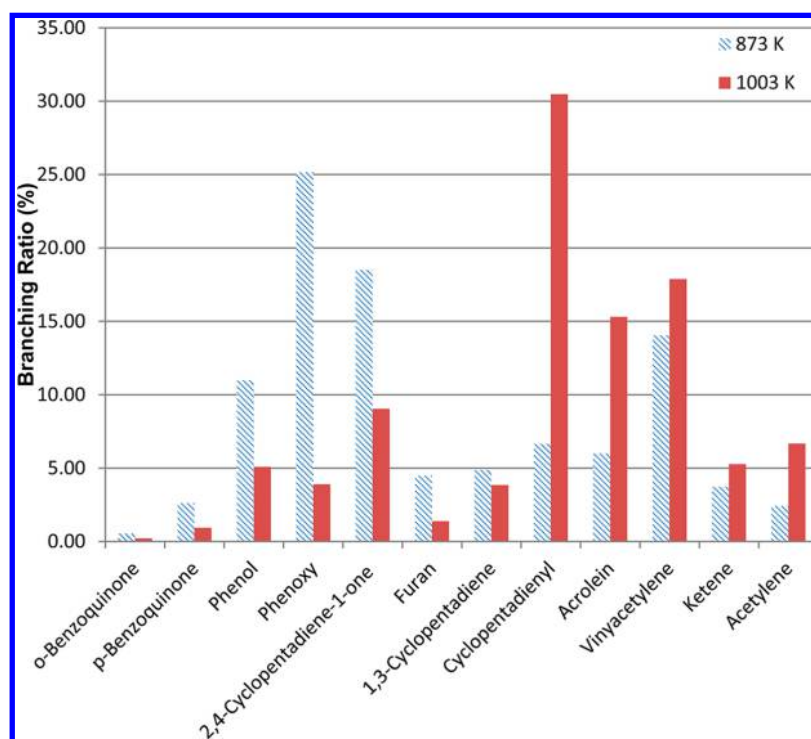


**Figure 4.** Branching ratio percentage for reaction of phenyl radicals with molecular oxygen at a pressure of 300 Torr at nozzle temperatures of 873 K (hatched column) and 1003 K (red column), as shown in Table 1

fashion to the cyclopentadienyl ( $C_5H_5$ ) spectrum at  $m/z$  65, the raw PIE for  $m/z$  66 shows a marked increase in photoionization efficiency slightly below 10 eV. We attribute this same characteristic PIE rise to dissociative ionization that is seen in the  $m/z$  66 signal in the pyrolysis of allylphenyl ether generating the phenoxy radical. Figure 2F shows the PIE at  $m/z$  66 after subtraction of this dissociative ionization signal. In the 1003 K experiment, there was also a small dissociative ionization contribution to the signal at  $m/z$  66 and subsequently subtracted from it. Here, the cyclopentadiene signal is of a similar magnitude to phenoxy radical and therefore could be expected to contribute to the signal. The resulting PIE at  $m/z$  66 is shown in Figure 3F and is well-fit by the cyclopentadiene ( $c-C_5H_6$ ) experimental reference PIE (red line).<sup>32</sup> It should be noted that 1,2,4-pentatriene with an ionization energy of 8.88 eV does not contribute to either signal. The linear molecules pent-3-yne and 3-pent-1-yne ( $l-C_5H_6$ ) have similar PIE onset as the signal at  $m/z$  66 but quickly plateau at 8.90 eV and therefore do not fit.

Finally, the PIE at  $m/z$  52 (Figures 2H and 3H) are well-matched with the reference spectrum for vinylacetylene ( $C_4H_4$ ),<sup>34</sup> and the PIE at  $m/z$  53 is the  $^{13}C$  signal of vinylacetylene ( $C_4H_4$ ) with no contribution from  $C_4H_5$ . The PIE at  $m/z$  42 (Figures 2I and 3I) matches the reference PIE for ketene ( $C_2H_2O$ ),<sup>31</sup> and the PIE collected at  $m/z$  26 (Figures 2K and 3K) shows good agreement with the reference PIE for acetylene ( $C_2H_2$ ).<sup>31</sup> The PIE of the signal at  $m/z$  56 (Figures 2J and 3J) are well-matched by the PIE of acrolein ( $C_3H_4O$ ) (red line).<sup>35</sup> The branching ratios percentage for each product peak ( $m/z = 108, 94, 93, 80, 68, 66, 65, 56, 52, 42,$  and 26) have been calculated along with error bars and shown in Table 1 and in Figure 4 for the reaction of phenyl radicals and molecular oxygen at 873 and 1003 K. The branching ratios were calculated based on integrated mass peaks primarily from the mass spectra depicted in Figure 1 at 10.5 eV. In the case of

acetylene, mass spectra at 12 eV were used along with the strong signal of vinylacetylene as a reference. The absorption cross sections used are referenced in Table 1.

#### IV. DISCUSSION

Having identified the products formed in the elementary reaction of the phenyl radical with molecular oxygen, we will now rationalize their formation pathways and propose a reaction mechanism (Figure 5). The phenyl plus molecular oxygen reaction was studied computationally using ab initio G2M calculations and will be used to rationalize the mechanism.<sup>9</sup> Initially a peroxybenzene radical intermediate is formed via a barrier-less addition of the phenyl radical to molecular oxygen. From peroxybenzene, the terminal peroxide oxygen migrates to the *ortho* carbon, from which a hydrogen atom is emitted to form *o*-benzoquinone.<sup>9</sup> Further migration of the oxygen atom to the *para* position leading to the formation of *p*-benzoquinone is practically negligible, according to calculations.<sup>9</sup> Furthermore, by this mechanism we would also expect to see formation of *m*-benzoquinone. Therefore, formation of *p*-benzoquinone is associated with a secondary reaction. The second pathway available to peroxybenzene involves an atomic oxygen emission to form the phenoxy radical. The phenoxy radical has been observed experimentally in single collision crossed beam reactions<sup>12–14</sup> and predicted as the primary reaction product theoretically, especially when approaching high temperatures of 1500–2500 K.<sup>8–10</sup> Finally, peroxybenzene can isomerize to a 2-oxepinoxy radical and subsequently emit a carbon dioxide molecule to form the cyclopentadienyl radical ( $C_5H_5$ ). Electronic structure calculations predict the cyclopentadienyl radical can be reached by a number of pathways, the two lowest-energy pathways pass through the seven-membered ring intermediate 2-oxepinoxy before undergoing rearrangement and carbon dioxide emis-

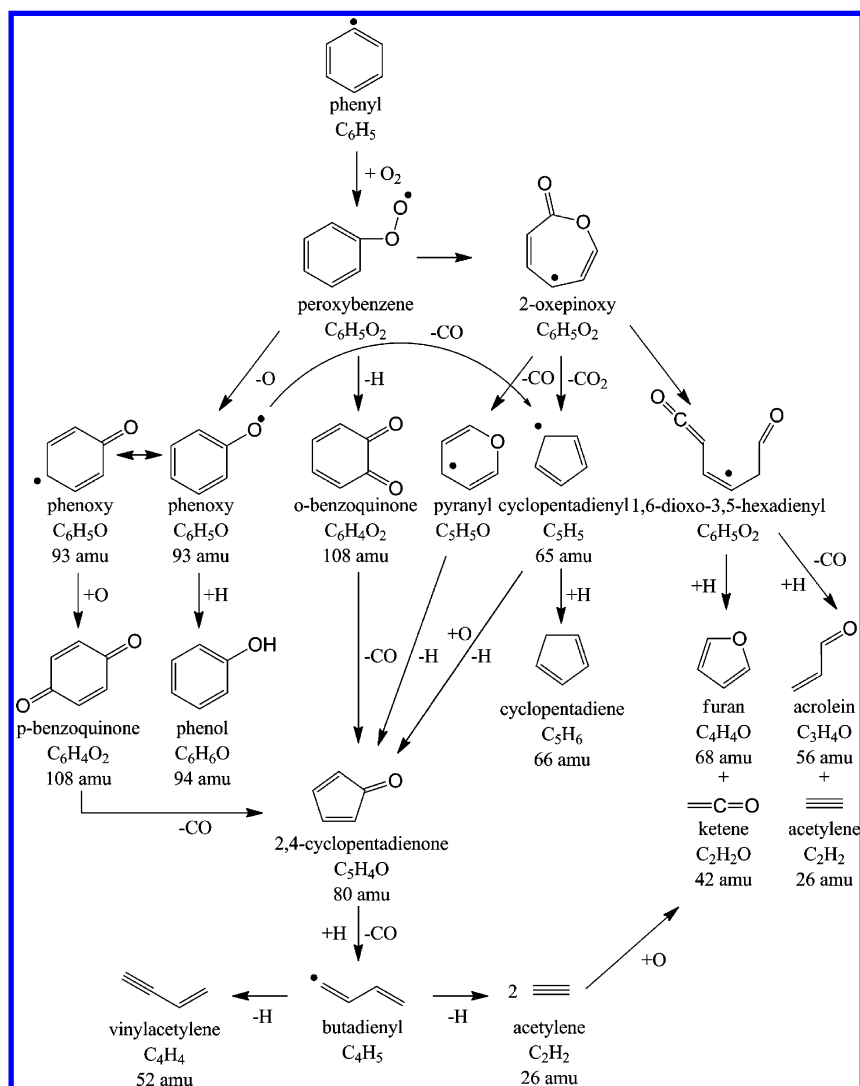


**Figure 5.** Proposed mechanism for products observed in the reaction of phenyl radicals with molecular oxygen at 300 Torr, 873 and 1003 K. Masses in amu have been given for the species observed in the experiments.<sup>9</sup>

sion.<sup>9</sup> The formation of cyclopentadienyl radical by carbon dioxide emission is calculated to be the most exoergic reaction channel, ranging from  $480 \text{ kJ mol}^{-1}$  below the energy of the reactants. The cyclopentadienyl radical is also accessible through a carbon monoxide (CO) emission from the phenoxy radical. Here, the ring structure is formed before carbon monoxide emission in a series of increasingly endoergic isomerization steps resulting in a reaction energy of  $38 \text{ kJ mol}^{-1}$  above the energy of the reactants.<sup>36,37</sup> The 2-oxepinoxy radical can undergo ring rupture to form a 1,6-dioxo-3,5-hexadienyl radical intermediate which can subsequently dissociate to form a range of polycarbon monoxide molecules and radicals.<sup>15</sup> These in turn can fragment further or undergo hydrogen addition or abstract a hydrogen atom.<sup>15</sup> Calculations show that 1,6-dioxo-3,5-hexadienyl radical intermediate can cyclize to furan ( $\text{C}_4\text{H}_4\text{O}$ ) and emit a ketene ( $\text{C}_2\text{HO}$ ) radical or emit carbon monoxide then fragment to acetylene and the acrolein radical ( $\text{C}_3\text{H}_3\text{O}$ ).<sup>15</sup> The ketene and acrolein radicals can easily undergo hydrogen atom addition or abstract one from another molecule as seen with the phenoxy and cyclopentadienyl radicals forming phenol and cyclopentadiene, to form ketene ( $\text{C}_2\text{H}_2\text{O}$ ) and acrolein ( $\text{C}_3\text{H}_4\text{O}$ ), respectively. The fragmentation of the 1,6-dioxo-3,5-hexadienyl radical and

2-oxepinoxy radicals can form furan ( $\text{C}_4\text{H}_4\text{O}$ ), ketene ( $\text{C}_2\text{H}_2\text{O}$ ), and acrolein ( $\text{C}_3\text{H}_4\text{O}$ ) directly along with a radical counterpart and are therefore considered primary reaction products. To conclude, the primary products formed in the reaction of the phenyl radical with molecular oxygen are *o*-benzoquinone plus atomic hydrogen (3), the phenoxy radical plus atomic oxygen (2), cyclopentadienyl radical plus carbon dioxide (5),  $\text{C}_4\text{H}_3\text{O}$  plus ketene, acrolein plus carbon monoxide and acetylene and furan plus ketene radical.

Having established the primary reaction products, we now explore the potential formation pathways to secondary and/or higher-order products. The phenoxy radical has resonant structures with carbon-centered radicals, of which the *para*-carbon-centered radical would be the most stable.<sup>38,39</sup> Reaction of a *para*-carbon-centered phenoxy radical with molecular oxygen followed by oxygen and hydrogen atom emissions could account for *para*-benzoquinone formation. The formation of phenol can be explained via hydrogen atom addition to the phenoxy radical; alternatively, the phenoxy radical can abstract a hydrogen atom from any hydrogen-bearing species. Previous combustion experiments found phenol formation whenever phenoxy radicals are generated.<sup>40</sup> The cyclopentadienyl radical can also undergo a hydrogen addition and/or abstraction to

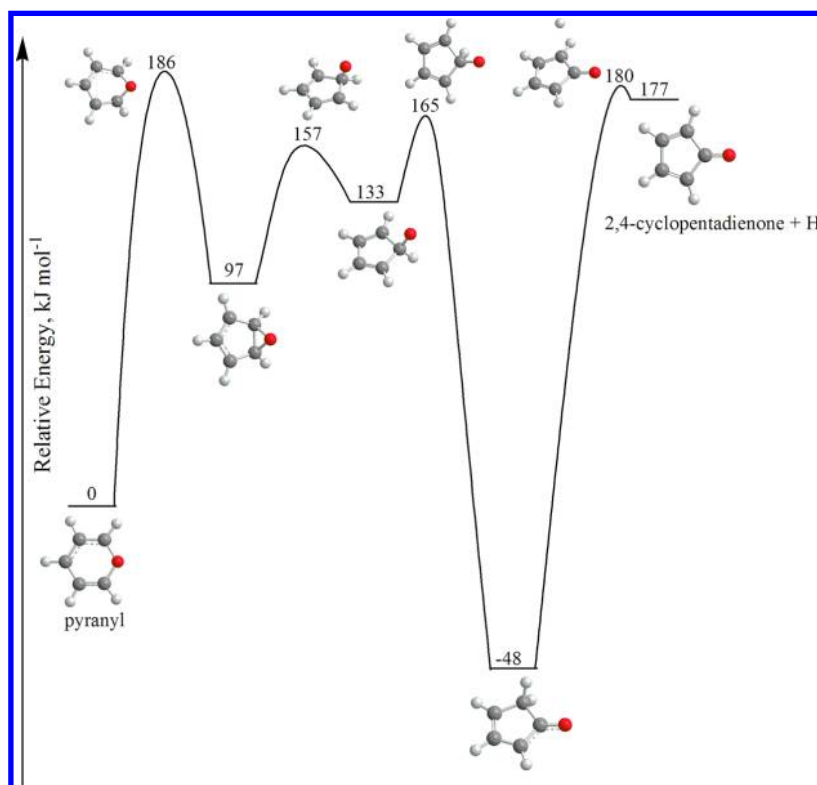


**Figure 6.** Potential energy diagram for decomposition of pyranyl to 2,4-cyclopentadienone + H calculated at the CCSD(T)/CBS(dtq)//B3LYP/6-311G\*\* + ZPE(B3LYP/6-311G\*\*) level of theory. Relative energies of various species are given in  $\text{kJ mol}^{-1}$ .

form cyclopentadiene.<sup>17</sup> The formation of 2,4-cyclopentadienone ( $\text{C}_5\text{H}_4\text{O}$ ) might be due to secondary decomposition of pyranyl as will be discussed later and is accessible through the reaction of cyclopentadienyl with atomic oxygen followed by atomic hydrogen loss or via the decomposition of benzoquinone through carbon monoxide emission which has been seen for *p*-benzoquinone decomposition.<sup>17</sup>

The final series of reactions involve carbon monoxide emission and/or ring openings to yield acyclic unsaturated hydrocarbons such as vinylacetylene ( $\text{C}_4\text{H}_4$ ) and acetylene ( $\text{C}_2\text{H}_2$ ). Glassman et al. predicted that the 2,4-cyclopentadienone ( $\text{C}_5\text{H}_5\text{O}$ ) radical can undergo decomposition via carbon monoxide emission to form a butadienyl radical ( $\text{C}_4\text{H}_5$ ), which then emits a hydrogen atom to form vinylacetylene.<sup>20</sup> The butadienyl radical intermediate can also dissociate via carbon-carbon cleavage to form acetylene plus a vinyl radical.<sup>20</sup> It should be noted the mass peak at  $m/z$  53 was solely from  $^{13}\text{C}$  isotope of vinylacetylene  $m/z$  52 and not from the butadienyl radical. Acetylene can undergo addition by an oxygen atom to form ketene. We did not observe pyranyl ( $\text{C}_5\text{H}_5\text{O}$ ) plus carbon monoxide (6) or 2-oxo-2,3-dihydrofuran-4-yl ( $\text{c-C}_4\text{H}_3\text{O}_2$ ) plus acetylene (7) reaction channels under our experimental conditions of 873 and 1003 K at 300 Torr. The pathway to 2-oxo-2,3-dihydrofuran-4-yl was predicted to be uncompetitive by the theoretical calculations.<sup>9,22</sup> On the contrary, the yield of pyranyl was anticipated to increase as the temperature decreases below 1500 K and hence be significant under the conditions of the present experiment. In order to explain the nonobservation of pyranyl, we computed its secondary decomposition pathway using the quantum chemical CCSD(T)/CBS(dtq)//B3LYP/6-311G\*\* method. The potential energy diagram is illustrated in Figure 6. One can see that pyranyl first undergoes ring contraction to a five-member ring

structure via an epoxylike intermediate and then loses an H atom to form 2,4-cyclopentadien-1-one after a hydrogen migration from C(O) to C(H). While the overall decomposition reaction is computed to be endothermic by  $177 \text{ kJ mol}^{-1}$ , the highest barrier on this pathway is at  $186 \text{ kJ mol}^{-1}$  above pyranyl. Meanwhile, the exothermicity of the  $\text{C}_6\text{H}_5 + \text{O}_2 \rightarrow \text{pyranyl} + \text{carbon monoxide}$  channel was computed to be as high as  $379 \text{ kJ mol}^{-1}$ .<sup>9</sup> If the primary pyranyl fragment is formed with that internal energy, its lifetime with respect to the decomposition to 2,4-cyclopentadien-1-one is computed to be only 0.3 ns using RRKM theory. The most probable kinetic energy of the primary fragments should resemble the reverse barrier height at the last step of decomposition of a  $\text{C}_6\text{H}_5\text{O}_2$  intermediate to pyranyl plus carbon monoxide, which is  $85 \text{ kJ mol}^{-1}$  according to the earlier calculations.<sup>9</sup> If we subtract this energy from the reaction exothermicity and assume that most of the available energy should be transferred to the internal energy of the larger pyranyl fragment, the energy available to pyranyl then would be  $294 \text{ kJ mol}^{-1}$ . In this case, the computed lifetime increases to 6 ns, which is still more than 3 orders of magnitude shorter than the residence time in the tube. Although some fraction of pyranyl molecules may be deactivated by collisions and thus survive longer, according to the experimental data, this fraction is not sufficient enough to be detected.

The branching ratios depicted in Figure 4 and listed in Table 1 deliver the relative weighting of decomposition pathways shown in Figure 5 and an insight into the role temperature plays in their determination. Although these data cannot provide quantitative information on the reaction mechanisms, we will briefly discuss the observed trends qualitatively and speculate on their origins. Overall, the 873 K experiment shows higher levels of high mass products, while the 1003 K



experiment shows an increase in lower mass products starting at the cyclopentadienyl radical ( $m/z$  65). Most likely, the reaction mechanism is being pushed down to low mass products through an increased amount of decomposition and fragmentation. The low-temperature experiment at 873 K provides a snapshot of the mechanism before reaching the final products. Interestingly, the cyclopentadienyl signal increases proportionately with the decrease in the phenoxy signal, indicating that although phenoxy is formed at higher temperatures it almost immediately decomposes to cyclopentadienyl and other products. The branching ratios of *o*-benzoquinone are about 0.25 of those of *p*-benzoquinone, indicating that the formation of the phenoxy radical by oxygen emission is preferential to formation of *o*-benzoquinone by hydrogen emission. The branching ratios of both benzoquinone isomers get proportionately lower with increasing temperature, a likely indicator of their thermal lability. The 2,4-cyclopentadiene-1-one signal shows about the same decrease of 0.5 with increased temperature as *o*-benzoquinone, indicating these pathways may be coupled, as shown in Figure 5. Alternatively, this observation corroborates the hypothesis that 2,4-cyclopentadiene-1-one is largely produced via secondary decomposition of pyranlyl because the primary yields of *o*-benzoquinone and pyranlyl show similar trends decreasing with temperature according to the RRKM-ME calculations.<sup>22</sup> Furan depicts a decrease with increased temperature, indicating it breaks down further at higher temperatures and is a primary product. Likewise, ketene shows a minimal relative rise with increased temperature. Acrolein on the other hand rises by a factor of 2.5 and most likely represents a terminal product of the reaction. Vinylacetylene shows only a marginal increase with temperature, while acetylene shows a greater increase. Vinylacetylene is a dominant product in the phenyl plus oxygen reaction which may well be degraded further to acetylene with increased temperature.

## V. CONCLUSION

A high-temperature chemical reactor was exploited to comprehensively investigate the primary and secondary products of the multichannel reaction of the phenyl radical with molecular oxygen under combustion relevant conditions (300 Torr, 873 and 1003 K), exploiting fragment-free photoionization of the neutral products. The formation of the primary products is initiated by the addition of molecular oxygen to the phenyl radical; the peroxybenzene radical intermediate reacts via three pathways ultimately forming: (i) *o*-benzoquinone ( $C_6H_4O_2$ ), (ii) the cyclopentadienyl radical ( $C_5H_5$ ), (iii) the phenoxy radical ( $C_6H_5O$ ), (iv) furan ( $C_4H_4O$ ), (v) acrolein ( $C_3H_4O$ ), and (vi) ketene ( $C_2H_2O$ ). Higher-order reaction products, phenol ( $C_6H_5OH$ ) and cyclopentadiene ( $C_5H_6$ ) are formed through a barrier-less atomic hydrogen addition to the phenoxy and cyclopentadienyl radical, respectively. 2,4-Cyclopentadienone ( $C_5H_4O$ ) may originate from decomposition of an unobserved primary fragment pyranlyl ( $C_5H_5O$ ), or from cyclopentadienyl addition to either atomic or molecular oxygen followed by emission of atomic hydrogen or OH (or atomic oxygen followed by atomic hydrogen), respectively, or through carbon monoxide emission from *o*-/*p*-benzoquinone. 2,4-Cyclopentadienone presents the central reaction intermediate leading to highly unsaturated carbons as the 2,4-cyclopentadienone radical degrades to vinylacetylene ( $C_4H_4$ ) through sequential carbon monoxide and atomic hydrogen emissions, yielding eventually vinyl-

acetylene and acetylene. We find no evidence of pyranlyl ( $C_5H_5O$ ) formation, which may be due to its fast secondary decomposition to 2,4-cyclopentadienone plus H.

Our results on the reaction of the phenyl radical with molecular oxygen, the prototype system leading to the degradation of aromatic radicals, highlight the importance of universal detection techniques in identifying isomer-specific product distributions produced within combustion environments comprehensively, rather than only select products. This method allows for experimental identification of hitherto elusive products and the elucidation of complete reaction networks. We anticipate that the present study acts as a conceptual template to initiate further investigations into the degradation pathways of more complex aromatic radicals by molecular oxygen exploiting fragment-free tunable vacuum ultraviolet photoionization. These reactions could involve, for instance, prototypes of bicyclic PAH radicals, the naphthyl ( $C_{10}H_7$ ) and indenyl ( $C_9H_7$ ) radicals. Additionally, this method could be expanded to more complex systems, such as nitrogen-substituted PAH radicals of biological importance relevant to DNA and RNA damage by ionizing radiation.

## ■ AUTHOR INFORMATION

### Corresponding Authors

\*E-mail: ralfk@hawaii.edu.

\*E-mail: MAhmed@lbl.gov.

\*E-mail: mebel@fiu.edu.

### Notes

The authors declare no competing financial interest.

## ■ ACKNOWLEDGMENTS

This material is based upon work supported by the U.S. Department of Energy, Office of Science, DE-FG02-03ER15411 to the University of Hawaii and DE-FG02-04ER15570 to FIU. The authors M.A., O.K., and T.P.T., and the Advanced Light Source are supported by the Director, Office of Science, Office of Basic Energy Sciences, of the U.S. Department of Energy under Contract DE-AC02-05CH11231, through the Chemical Sciences Division. A.M.M. would like to acknowledge the Instructional & Research Computing Center (IRCC, web: <http://ircc.fiu.edu>) at FIU for providing HPC computing resources that have contributed to the research results reported within this paper.

## ■ REFERENCES

- (1) Baird, W. M.; Hooven, L. A.; Mahadevan, B. Carcinogenic Polycyclic Aromatic Hydrocarbon-DNA Adducts and Mechanism of Action. *Environ. Mol. Mutagen.* **2005**, *45*, 106–114.
- (2) Finlayson-Pitts, B. J.; Pitts, J. N., Jr. Tropospheric Air Pollution: Ozone, Airborne Toxics, Polycyclic Aromatic Hydrocarbons, and Particles. *Science (New York, N.Y.)* **1997**, *276*, 1045–1052.
- (3) Frenklach, M. Reaction Mechanism of Soot Formation in Flames. *Phys. Chem. Chem. Phys.* **2002**, *4*, 2028–2037.
- (4) Richter, H.; Howard, J. B. Formation and Consumption of Single-Ring Aromatic Hydrocarbons and Their Precursors in Premixed Acetylene, Ethylene and Benzene Flames. *Phys. Chem. Chem. Phys.* **2002**, *4*, 2038–2055.
- (5) Parker, D. S. N.; Zhang, F.; Kim, Y. S.; Kaiser, R. I.; Landera, A.; Kislov, V. V.; Mebel, A. M.; Tielens, A. G. G. M. Low Temperature Formation of Naphthalene and Its Role in the Synthesis of PAHs (Polycyclic Aromatic Hydrocarbons) in the Interstellar Medium. *Proc. Natl. Acad. Sci. U.S.A.* **2012**, *109*, 53–58.
- (6) Kaiser, R. I.; Parker, D. S. N.; Zhang, F.; Landera, A.; Kislov, V. V.; Mebel, A. M. PAH Formation under Single Collision Conditions:

Reaction of Phenyl Radical and 1,3-Butadiene to Form 1,4-Dihydronaphthalene. *J. Phys. Chem. A* **2012**, *116*, 4248–4258.

(7) Parker, D. S. N.; Zhang, F.; Kaiser, R. I.; Kislov, V. V.; Mebel, A. M. Indene Formation under Single-Collision Conditions from the Reaction of Phenyl Radicals with Allene and Methylacetylene-a Crossed Molecular Beam and Ab Initio Study. *Chem.–Asian J.* **2011**, *6*, 3035–3047.

(8) Barckholtz, C.; Fadden, M. J.; Hadad, C. M. Computational Study of the Mechanisms for the Reaction of O<sub>2</sub> with Aromatic Radicals. *J. Phys. Chem. A* **1999**, *103*, 8108–8117.

(9) Tokmakov, I. V.; Kim, G.-S.; Kislov, V. V.; Mebel, A. M.; Lin, M. C. The Reaction of Phenyl Radical with Molecular Oxygen: A G2M Study of the Potential Energy Surface. *J. Phys. Chem. A* **2005**, *109*, 6114–6127.

(10) Yu, T.; Lin, M. C. Kinetics of the C<sub>6</sub>H<sub>5</sub> + O<sub>2</sub> Reaction at Low Temperatures. *J. Am. Chem. Soc.* **1994**, *116*, 9571–9576.

(11) Fadden, M. J.; Barckholtz, C.; Hadad, C. M. Computational Study of the Unimolecular Decomposition Pathways of Phenylperoxy Radical. *J. Phys. Chem. A* **2000**, *104*, 3004–3011.

(12) Parker, D. S. N.; Zhang, F.; Kaiser, R. I. Phenoxy Radical (C<sub>6</sub>H<sub>5</sub>O) Formation under Single Collision Conditions from Reaction of the Phenyl Radical (C<sub>6</sub>H<sub>5</sub>) with Molecular Oxygen (O<sub>2</sub>): The Final Chapter? *J. Phys. Chem. A* **2011**, *115*, 11515–11518.

(13) Albert, D. R.; Davis, H. F. Collision Complex Lifetimes in the Reaction C<sub>6</sub>H<sub>5</sub> + O<sub>2</sub> → C<sub>6</sub>H<sub>5</sub>O + O. *J. Phys. Chem. Lett.* **2010**, *1*, 1107–1111.

(14) Gu, X.; Zhang, F.; Kaiser, R. I. Crossed Beam Reaction of the Phenyl Radical, (C<sub>6</sub>H<sub>5</sub>, X<sup>2</sup>A') with Molecular Oxygen (O<sub>2</sub>, X<sup>3</sup>σ<sup>-G</sup>): Observation of the Phenoxy Radical, (C<sub>6</sub>H<sub>5</sub>O, X<sup>2</sup>A'). *Chem. Phys. Lett.* **2007**, *448*, 7–10.

(15) Fadden, M. J.; Hadad, C. M. Unimolecular Decomposition of the 2-Oxepinoxy Radical: A Key Seven-Membered Ring Intermediate in the Thermal Oxidation of Benzene. *J. Phys. Chem. A* **2000**, *104*, 8121–8130.

(16) Merle, J. K.; Hadad, C. M. Computational Study of the Oxygen Initiated Decomposition of 2-Oxepinoxy Radical: A Key Intermediate in the Oxidation of Benzene. *J. Phys. Chem. A* **2004**, *108*, 8419–8433.

(17) Frank, P.; Herzler, J.; Just, T.; Wahl, C. High-Temperature Reactions of Phenyl Oxidation. *Symp. (Int.) Combust., [Proc.]* **1994**, *25*, 833–840.

(18) Herzler, J.; Frank, P. In *Third International Conference on Chemical Kinetics*, Gaithersburg, MD, July 12–16, 1993; Vol. 3.

(19) Carpenter, B. K. Computational Prediction of New Mechanisms for the Reaction of Vinyl and Phenyl Radicals with Molecular Oxygen. *J. Am. Chem. Soc.* **1993**, *115*, 9806–9807.

(20) Venkat, C.; Brezinsky, K.; Glassman, I. High Temperature Oxidation of Aromatic Hydrocarbons. *Symp. (Int.) Combust., [Proc.]* **1982**, *19*, 143–152.

(21) Belmekki, N.; Glaude, P. A.; Da Costa, I.; Fournet, R.; Battin-Leclerc, F. Experimental and Modeling Study of the Oxidation of 1-Butyne and 2-Butyne. *Int. J. Chem. Kinet.* **2002**, *34*, 172–183.

(22) Kislov, V. V.; Singh, R. I.; Edwards, D. E.; Mebel, A. M.; Frenklach, M. Rate Coefficients and Product Branching Ratios for the Oxidation of Phenyl and Naphthyl Radicals: A Theoretical RRKM-ME Study. *Proc. Int. Combust. Inst.* **2014**, [Online early access]. DOI: 10.1016/j.proci.2014.06.135 (accessed July 28, 2014).

(23) Kohn, D. W.; Clauberg, H.; Chen, P. Flash Pyrolysis Nozzle for Generation of Radicals in a Supersonic Jet Expansion. *Rev. Sci. Instrum.* **1992**, *63*, 4003–4005.

(24) Nicolas, C.; Shu, J.; Peterka, D. S.; Hochlaf, M.; Poisson, L.; Leone, S. R.; Ahmed, M. Vacuum Ultraviolet Photoionization of C<sub>3</sub>. *J. Am. Chem. Soc.* **2006**, *128*, 220–226.

(25) Golan, A.; Ahmed, M.; Mebel, A. M.; Kaiser, R. I. A Vuv Photoionization Study on the Multichannel Reaction of Phenyl Radicals with 1,3-Butadiene under Combustion Relevant Conditions. *Phys. Chem. Chem. Phys.* **2013**, *15*, 341–347.

(26) Zhang, F.; Kaiser, R. I.; Golan, A.; Ahmed, M.; Hansen, H. A VUV Photoionization Study of the Combustion-Relevant Reaction of the Phenyl Radical (C<sub>6</sub>H<sub>5</sub>) with Propylene (C<sub>3</sub>H<sub>6</sub>) in a High

Temperature Chemical Reactors. *J. Phys. Chem. A* **2012**, *116*, 3541–3546.

(27) Zhang, F.; Kaiser, R. I.; Kislov, V. V.; Mebel, A. M.; Golan, A.; Ahmed, M. A VUV Photoionization Study of the Formation of the Indene Molecule and Its Isomers. *J. Phys. Chem. Lett.* **2011**, *2*, 1731–1735.

(28) Yang, J. *Photonization Cross Section Database*, version 1.0; 2011.

(29) Li, Y. *Photonization Cross Section Database*, version 1.0; 2011.

(30) Sander, W.; Roy, S.; Polyak, I.; Ramirez-Anguita, J. M.; Sanchez-Garcia, E. The Phenoxy Radical–Water Complex—A Matrix Isolation and Computational Study. *J. Am. Chem. Soc.* **2012**, *134*, 8222–8230.

(31) Yang, B.; Wang, J.; Cool, T. A.; Hansen, N.; Skeen, S.; Osborn, D. L. Absolute Photoionization Cross-Sections of Some Combustion Intermediates. *Int. J. Mass Spectrom.* **2012**, *309*, 118–128.

(32) Hansen, N.; Klippenstein, S. J.; Miller, J. A.; Wang, J.; Cool, T. A.; Law, M. E.; Westmoreland, P. R.; Kasper, T.; Kohse-Hoeinghaus, K. Identification of C<sub>3</sub>H<sub>x</sub> Isomers in Fuel-Rich Flames by Photoionization Mass Spectrometry and Electronic Structure Calculations. *J. Phys. Chem. A* **2006**, *110*, 4376–4388.

(33) Xu, H.; Pratt, S. T. Photodissociation of Anisole and Absolute Photoionization Cross-Section of the Phenoxy Radical. *J. Phys. Chem. A* **2013**, *117*, 12075–12081.

(34) Cool, T. A.; Wang, J.; Nakajima, K.; Taatjes, C. A.; McIlroy, A. Photoionization Cross Sections for Reaction Intermediates in Hydrocarbon Combustion. *Int. J. Mass Spectrom.* **2005**, *247*, 18–27.

(35) Goulay, F.; Trevitt, A. J.; Savee, J. D.; Bouwman, J.; Osborn, D. L.; Taatjes, C.; Wilson, K. R.; Leone, S. R. Product Detection of the CH Radical Reaction with Acetaldehyde. *J. Phys. Chem. A* **2012**, *116*, 6091–6106.

(36) Colussi, A. J.; Zabel, F.; Benson, S. W. The Very Low-Pressure Pyrolysis of Phenyl Ethyl Ether, Phenyl Allyl Ether, and Benzyl Methyl Ether and the Enthalpy of Formation of the Phenoxy Radical. *Int. J. Chem. Kinet.* **1977**, *9*, 161–178.

(37) Lin, C.-Y.; Lin, M. C. Thermal Decomposition of Methyl Phenyl Ether in Shock Waves: The Kinetics of Phenoxy Radical Reactions. *J. Phys. Chem.* **1986**, *90*, 425–431.

(38) Buth, R.; Hoyermann, K.; Seeba, J. Reactions of Phenoxy Radicals in the Gas Phase. *Symp. (Int.) Combust., [Proc.]* **1994**, *25*, 841–849.

(39) Liu, R. F.; Morokuma, L.; Mebel, A. M.; Liu, M. C. Ab Initio Study of the Mechanism for the Thermal Decomposition of the Phenoxy Radical. *J. Phys. Chem.* **1996**, *100*, 9314–9322.

(40) Taatjes, C. A.; Osborn, D. L.; Selby, T. M.; Meloni, G.; Trevitt, A. J.; Epifanovsky, E.; Krylov, A. I.; Sirjean, B.; Dames, E.; Wang, H. Products of the Benzene + O(<sup>3</sup>p) Reaction. *J. Phys. Chem. A* **2010**, *114*, 3355–3370.